MEMS for Space Applications

Linda M. Miller[1]
Jet Propulsion Laboratory, MS 302-306, 4800 Oak Grove Dr., Pasadena, CA 91109

ABSTRACT

The future of robotic space missions is in ever-smaller platforms and MicroElectroMechanical Systems (MEMS) will be key in this development. New measurement schemes may be required instead of brute-force miniaturization of current instruments. Trade-offs between mass and sensitivity need to be addressed in mission planning. Suites of sensors may replace large, highly sensitive macro-instruments. E.g. MEMS-based microgyros currently have higher drift rates than spinning mass gyros used in Cassini-like missions, but used in conjunction with microaccelerometers, star-trackers or sun-sensors, provide capable inertial navigation systems. Therefore, the "system" aspect of MEMS is essential for the trend towards micromissions. Sensor interfaces must be designed for flight. Packaging likewise needs to be considered part of the system. CAD and simulations tools will be required for the entire system: electronics, sensor (and/or actuator), and package. Thermal, mechanical, and electrical analysis under harsh conditions will be required. For space applications, MEMS devices must be flight qualified for vibration, shock, radiation, temperature, vacuum specifications and must meet reduced mass, power, and volume budgets. MEMS reliability is essential for space applications. Long lifetimes, self-test, self-calibration, and potentially evolvable systems need to be created. Packaging of MEMS must protect devices from harsh environments; packaging needs to be included in sensor/actuator development.

Keywords: MEMS, Space, Review

1. INTRODUCTION

It is increasingly difficult to find public support for the large-scale space missions, which have been typical of the previous three decades. Reducing mission costs is key to the development of support for future missions and the science return they can generate. The space science community is exploring many avenues for the reduction of mission costs, including international cooperation on missions, increased spacecraft autonomy, smaller missions and spacecraft, reduced mission goals, etc. The use of technological developments such as MicroElectroMechanical Systems (MEMS) is particularly attractive because it provides an avenue for the reduction of mission costs without the sacrifice of mission capability.

How do MEMS fit into this development? MEMS provide the necessary tools for miniaturization of mechanical transducers and actuators critical for science and engineering objectives while meeting the size limitations of this new class of microspacecraft. Miniaturization of platforms to perform these measurements requires high performance, low mass/volume, and low power.

Mass reductions are particularly important for mission cost reductions. For example, reducing the mass launched for an interplanetary mission by a factor of 10X allows the use of a Delta II launch vehicle instead of a Titan IV B, a savings of approximately $400,000,000 U.S. dollars. This is a saving in launch costs alone. Reducing the overall mass budget of a mission can be accomplished by reducing the instrument size using MEMS-based microinstruments. This not only reduces the instrument mass, but also reduces the support structure on which the instrument is bolted to the spacecraft. This spacecraft bus is often the significant mass overhead of the spacecraft. Large mass reductions also enable the development of so-called "micro- and nano-missions", which are being designed with more and more sophisticated science objectives, and are often being launched in a "piggyback" configuration. In this mode, the micro-mission may be considered "ballast" for the larger primary payload. In this case, every gram counts. Every bit of performance that can be squeezed from the subsystems (read MEMS) is essential for the overall mission success.

This paper will review some examples of current missions which rely on MEMS for science measurements, highlight some of the unique requirements of MEMS for space applications, explore some examples of current MEMS and the ways in which MEMS can reduce mission costs, and finally, examine the ultimate in spacecraft miniaturization using MEMS technologies.

[1] Correspondence: Email: Linda.M.Miller@jpl.nasa.gov Telephone: 818-354-0982; FAX: 818-393-4540

2. MOTIVATION FOR MEMS IN SPACE APPLICATIONS: THE MICROMISSION

2.1 Mass and Cost Considerations

It is increasingly difficult to find public support for the large-scale space missions that have been typical of the previous three decades. Reducing mission costs is key to the development of future missions and the science return necessary to excite the public. One major way to reduce mission costs is to reduce launch costs. For example, reducing the mass launched for an interplanetary mission from 7800 kg to 750 kg allow the use of a Delta II launch vehicle instead of a Titan IV B, a savings of approximately $400,000,000 U.S. dollars. This is a savings in launch only! It might appear that using a MEMS device has zero impact on the mass budget when considering a 750 kg payload, giving unlimited freedom in instrument design, but this is not the case, in part because of the significant overhead of the spacecraft bus, which typically scales with the instrument. Also, so-called "micro-missions" are now designed with more and more sophisticated science objectives, and are often being launched in a "piggyback" configuration. In this mode, the micro-mission is often considered "ballast" for the larger primary payload. In this case, every gram counts. Every bit of performance that can be squeezed from the subsystems is essential for the overall mission success.

2.2 Mars Microprobe: Micro-mission Example

An excellent example of this new type of micro-mission is the Mars Microprobe, which was developed by NASA's New Millenium [check spelling of millenium] Program and launched on January 3, 1999. The Mars Microprobe pioneers a new era of "network science" in which multiple probes or microspacecraft are distributed throughout a planet (or space, or throughout a crewed spacecraft) to monitor global meteorological, seismic, mineralogical, etc., phenomena. The Mars Microprobe, shown schematically in Figure X2, is composed of a forebody (<670 grams), tethered to an aftbody (~1.7 kg) and protected through entry into the Martian atmosphere by an aeroshell capable of withstanding up to 3000°F. Two Microprobes will arrive with the Mars Polar Lander at the Red Planet on December 3, 1999. The Microprobes are slowed from initial velocities of 7 km/sec to a final impact velocity of 200 m/sec by the non-ablative aeroshell, which also provides thermal insulation. During the descent of the probe through the Martian atmosphere, a sharp deceleration caused by atmospheric drag will be monitored by an Analog Devices single axis [actually a dual axis device which unfortunately has only one axis connected] ADXL50 micromachined accelerometer in the aftbody. The acceleration data will provide performance data on the aeroshell and give scientists clues to atmospheric density, temperature and pressure as a function of altitude. On impact with the Martian surface, the forebody and the aftbody separate, with the forebody penetrating to a depth of 0.3 – 1 meter, depending on the soil type, and the aftbody remaining with a few cm of the surface. The aftbody is designed to withstand an impact of 60,000 G and the normal Martian temperature range of 0 to –110C[not sure of exact number, but less than –80]. It supports a primary lithium battery source, descent accelerometer, solar cell experiment, and telecommunications module. The forebody measures the penetration impact, again with a MEMS-based accelerometer, in order to study the density and perhaps striations in the Martian soil. It can withstand a 0 to-120C temperature range, and 30,000 G's of impact deceleration. The forebody houses a microcontroller, power electronics, a tunable diode laser experiment to search for water, a soil conductivity experiment using thermistors and a sample collection drill and motor (See Figure X3). The overall mass of the Mars Microprobe including the aeroshell is less than 3.6 kg, and the total power resource is approximately 9 W-hrs.

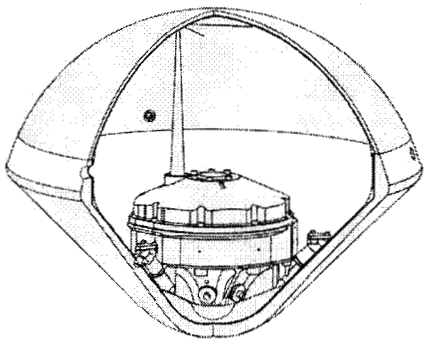

a.

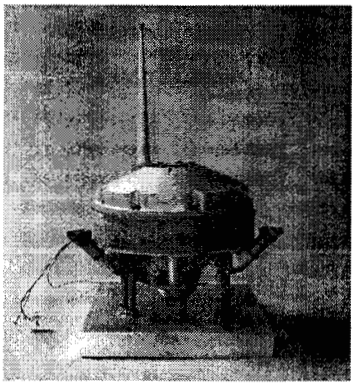

b.

Figure X2 (a) Schematic of Mar Microprobe housed in a protective aeroshell. (b) Photograph of Mars Microprobe forebody and aftbody.

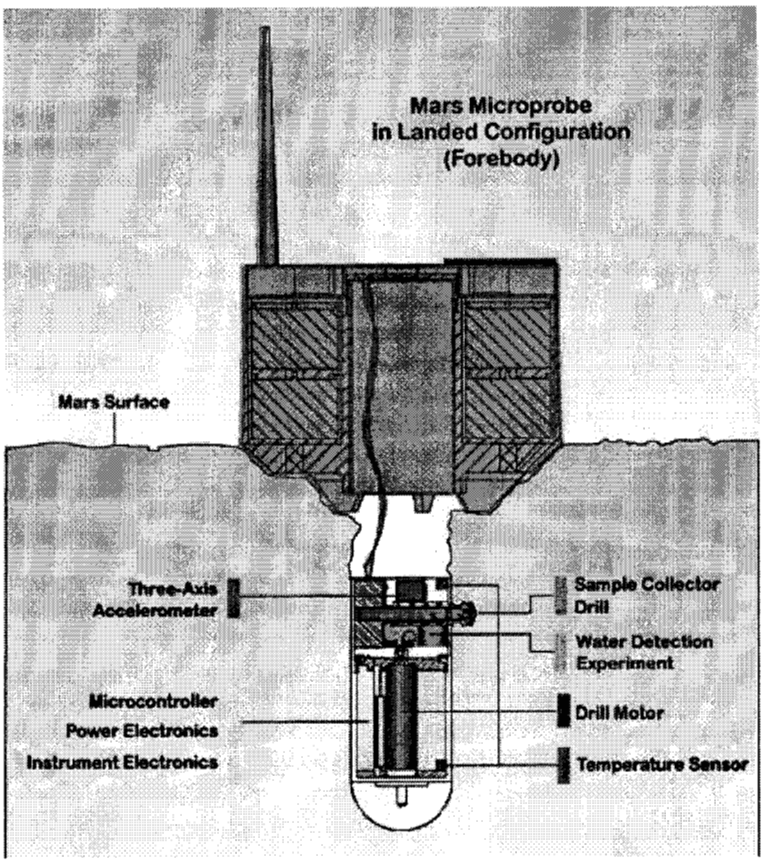

Figure X3 Schematic of Mars Microprobe following penetration of Martian surface. The forebody is tethered to a aftbody at the surface which communicates with the Mars Global Surveyor.

The Mars Microprobe is an excellent example of the direction of future space exploration and the potential role of MEMS in this future.

3. MEMS SPACE FLIGHT CONSIDERATIONS

3.1 MEMS Reliability

Outstanding advancements in MEMS device performance, mass, volume and power reduction, and overall system integration have made MEMS key in the development of micro- and nano-spacecraft. However, rapid insertion of MEMS into space applications will require parallel developments in MEMS reliability, packaging and flight qualification. To assist the MEMS community in these developments, the NASA's Jet Propulsion Laboratory (JPL) has produced the "MEMS Reliability Assurance Guidelines for Space Applications.[R1] This is a comprehensive review of issues from MEMS processing and structures to flight qualification of MEMS technologies. Highlights from this work are presented in this section.

MEMS device reliability is one of the most challenging areas in inserting MEMS into space applications. For example, device reliability is typically modeled using accelerated life-testing. However, since the failure modes in most MEMS devices are not well understood, life-testing is not very useful. However, several areas of failure modes and mechanisms have been defined and researched. These areas include both degradation failures and catastrophic failures. Some examples of failure modes and mechanisms include:

- Mechanical fracture (ductile, brittle, and intercrystalline) which is caused by stress to the device beyond its fracture strength
- Fatigue which is caused by cyclical stressing of the part [R2]

- Stiction [R3] caused by the contact of two very smooth surfaces and often promotes adhesion by van der Waals forces
- Wear caused by adhesion, abrasion, corrosion, and/or surface fatigue when two surface rub against one another
- Delamination caused by process contamination or mismatches in thermal expansion coefficients (CTE's) between two adjacent materials
- Environmentally Induced Failures (vibration, shock, humidity, radiation, particulates, temperature changes, electrostatic discharge) [R4]-[R6]
- Stray Stresses inherent
- Parasitic Capacitances

Many of these failure mechanisms can be understood through materials properties. However, bulk parameters do not precisely describe thin film parameters. In addition, thin film properties are process-dependent; but processes are generally a function of system parameters, which vary from laboratory to laboratory. This complexity of current MEMS development requires that processes as well as finished devices must be characterized and monitored carefully. This is often not the case in the rapidly changing designs of the MEMS researcher. However, for space applications, this approach is critical.

MEMS reliability will also improve as design techniques and tools develop. Finite element analysis can be used to analyze heat transfer, thermal stresses, thermal fatigue, and static and modal characteristics of a design prior to fabrication. This analysis can now be incorporated into several commercial packages for circuit design. As models and simulations improve, reliability of design will also improve.

3.2 MEMS Packaging

Reduction of size and cost of the space system requires an in depth look at packaging of MEMS devices. The package often determines a primary mass contributor to the MEMS device as well as an efficient (or inefficient) signal (ac, dc, RF) and energy transfer to and from the MEMS device. Likewise, the MEMS package provides heat transfer to and from the device, as well as protection from the environment, including radiation, humidity, mechanical, and/or electromagnetic protection. In essence, the package must be considered part of the overall system design.

MEMS packaging efforts have typically followed semiconductor packaging technologies with mixed results. Metal packages such as Cu/W (10/90), Silvar™ (a Ni-Fe alloy), CuMo (15/85), and CuW (15/85) are all excellent thermal conductors and have coefficients of thermal expansion (CTE's) compatible with silicon-based MEMS structures. Care must be taken, however, with metal packages to carefully remove any gases, such as H_2O or H_2, trapped during package fabrication. This is especially important for vacuum packaging of vibratory MEMS structures since device performance degrades under damping conditions.

Other packaging options include ceramic packages, thin-film multilayer packages using polyimide laminates, and plastic packages. Each type of package has its benefits and disadvantages in space applications. For example, a low temperature co-fired ceramic (LTCC) package can be cured at lower temperatures than conventional ceramics; however, care must be taken in choosing interconnection metals. Silver has been found to migrate during high temperature cycling and humid environments. Plastic packages, although inexpensive, are not hermetic and tend to crack in humid environments. Wafer-level packaging technologies are a clear need in MEMS development for space applications, especially for vacuum packaging requirements.

Die-attach is another critical factor in packaging of space MEMS. Solders, adhesive, and epoxies are typically used in MEMS packages. The die-attach must have good thermal conductivity; mechanically support (with minimal stress) the device during vibration, shock and acceleration; withstand thermal variations and possibly humid environments; and be compatible with device performance (e.g. minimal outgassing properties when used with sensitive MEMS devices).

Interconnect technology has advanced beyond manual wirebonds to "flip chip" methodologies. IBM first developed the controlled chip connection (C4), or flip-chip, in the 1960s. In this technology, solder bumps are used to connect wettable pads on the chip and substrate. This technology has many advantages. For example, solder bumps are self-aligning structures since only the chip pads are wettable. Likewise, built-in redundancy can minimize noise and improve fault tolerance. In addition, this technique is inherently reworkable. Stress on the interconnections during shock, vibration, mechanical stress, or thermal variations can be accommodated using chip underfill. Fluxless flip-chip methods have also been developed to improve reliability and compatibility with vacuum packaging. [R7]

In the near-term, i.e. prior to full-scale integration of MEMS with a spacecraft, multi-chip module packaging strategies are available and being improved. Multi-chip Modules (MCM's) and High Density Interconnects (HDI's) [R8] have been used for the integration of MEMS and electronics. Chip on Flex (COF) [R9]-[R10] has been modified to incorporate MEMS structures.

The final factor in packaging MEMS structures is the incorporation of test chips. The Multi-User MEMS Processes (MUMPS) [R11] offers test chips for surface micromachined structures. These chips include breakage detectors that monitor stress on the die, and polysilicon resistors that monitor heat in the package. Other test chips can be used to monitor process related issues such as stress in the layers or mask alignment. Similar test chips can be incorporated into bulk micromachined designs.

3.3 Flight Qualification

Flight qualification of macroscopic instruments has typically followed a strict regime of design, process, device, subsystem, and system verification and validation specific to launch vehicles and mission specifications. Although aspects of this methodology can be applied to MEMS, time and cost considerations of new missions require new ways of flight qualifying MEMS. As discussed previously, reliability is a challenging issue with MEMS. However, protocols [R1] have been developed which include process qualification, product qualification, product assurance, and company certification for commercial venues. Process qualification includes such standards as parametric monitoring, design rule development, technology characterization and standard evaluation test structures. Product qualification covers issues of design verification and product characterization. Product characterization will likely include thermal and mechanical characterization, as well as ESD sensitivity, voltage ramp, temperature ramp, and high/low temperature cycling. Additional testing may also be incorporated into flight qualification depending on the mission environment. Extreme conditions and associated mission destinations are outlined in Table 1.

Table 1 Mission Specific Environments

	Mars	Venus	Europa
Mean temperature			
Thermal range			
Radiation Environment			
Corrosives			

3.4 Summary

Much is still unknown in the area of MEMS reliability and current packaging technologies may be unsuitable for various MEMS devices. For example, soil sample microanalysis systems must be in contact with harsh environments; this presents special requirements for both life-testing and packaging. On the other hand, in vibratory devices Q-amplification of detected signals is tightly coupled to damping factors and thereby requires highly reliable vacuum packaging. Therefore, continuous development of MEMS reliability and MEMS packaging must be pursued in parallel with the outstanding advancements in device performance; mass, volume and power reduction; and system integration.

4. AN EXAMPLE OF MEMS FOR SPACE APPLICATIONS: MICRO INERTIAL REFERENCE SYSTEMS (μIRS)

Microspacecraft are 10-1000 smaller than Galileo or Cassini-type spacecraft. Therefore mass, volume, and power reduction in the navigation system is critical. For historical reference, a Cassini Inertial Reference System (circa 1980, a hemispherical-resonator gyroscope-based system developed by Delco/Litton) is 5 kg for 4 axes, ~28 X 20 X 10 cm^3, ~18 Watts, with a capture rate of 10 degrees/second (maximum rating), and a drift of 0.01 degrees/hour. In contrast, a MEMS-based micro-inertial reference system (μIRS), shown conceptually in figure 1, is projected to have the following attributes:

- low mass (<5.0g; 4,000 X reduction),
- low volume (1cm x 1cm x 0.2cm; 90,000X reduction),
- high performance (Microgyro goal: < 1 deg/hr bias stability, microaccelerometer goal: < 1 micro-g resolution),
- low power consumption (< 0.2 Watt; 100X reduction),
- inexpensive (< $10K; >>25X reduction),
- long lifetime (>20 years; >2 X increase),
- reduced electronics (1 chip; >10 X reduction),

- short turn-on time (< 1 sec),
- and radiation hardened.

Applications of the μIRS include small, low-cost spacecraft and satellites, micro-rovers, micro-probes, micro-aquatic missions, etc. Specific functions of this technology include attitude and maneuver control, pointing stabilization, and tumble recovery are all potential applications of this technology.

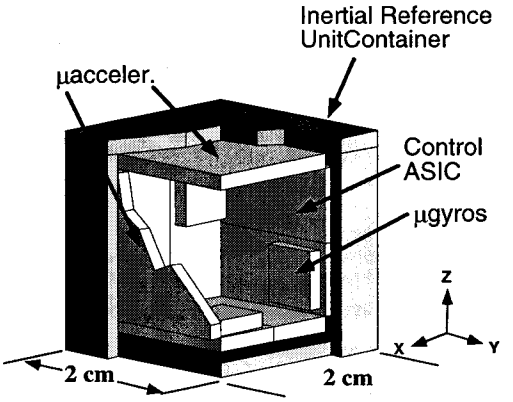

Figure 1. Conceptual schematic of a micro inertial reference system (μIRS) for microspacecraft applications. MEMS-based microgyros and microaccelerometers are controlled and monitored by a single-chip control ASIC.

To achieve the goals of a μIRS, MEMS-based vibratory gyroscopes [refs] have been demonstrated with drifts in the 1-100 degrees/hour range with <30 grams total mass, and with power consumption as small as 0.5 W for the entire package. One such example of a MEMS microgyroscope is being developed at NASA's Jet Propulsion Laboratory [references], with the express goal of producing a flight qualifiable μIRS. The JPL microgyro is shown in Figure 2. This device is bulk micromachined entirely from silicon. The three main components are the "clover-leaf, the silicon baseplate and the silicon post. The "cloverleaf is a symmetric structure with degenerate resonant modes about the x- and y-axes. The 4 petals of the "clover-leaf" also form a large area for electrostatic actuation and capacitive transduction of the drive and sensing modes, respectively. The silicon baseplate is Au/Au thermo-compression bonded to the support frame of the "clover-leaf" and also supports some sensor interface electronics to the external control system. The silicon post is assembled with the bonded "clover-leaf"/baseplate combination and produces a Coriolis force coupling between the drive and sensing modes (rocking modes about the x- and y-axes) when there is rotation about the post axis (see schematic in Figure 2 for axes definitions). By designing a minimal frequency shift between the two degenerate rocking modes, and driving the device on resonance, Q amplification of the sense single is possible. The device is sealed in a 10-100 mTorr environment for optimal performance.

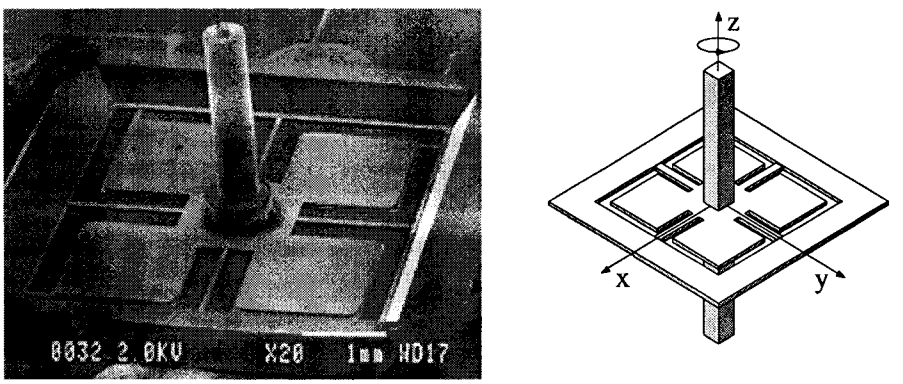

Figure 2. Scanning Electron Micrograph and corresponding schematic of JPL's vibratory microgyroscope. The vertical post is a Coriolis force transducer which causes a coupling between degenerate rocking modes (about the x and y axes) in the cloverleaf structure proportional to rotation about the z axis.

A block diagram of the microgyroscope under closed-loop control is shown in Figure 3. In this figure, the clover-leaf structure is represented by the dark squares. As described above, one of the degenerate rocking modes (e.g. about the x-axis) is driven on resonance and referred to as the "drive mode." This mode is monitored through the summing amplifier and fed back into an automatic gain control to set peak-to-peak oscillations of the drive mode. The difference amplifier picks up the "sense mode" (e.g. corresponding rocking mode about the y-axis) when there is rotation about the z-axis. This signal is typically small compared to the drive signal and is therefore monitored synchronously 90 deg out of phase with the drive signal to eliminate deleterious effects of noise and parasitic capacitances. The advantages of this configuration include the simplicity of the electronics, which are partly due to the symmetries in the mechanical design of the microgyroscope, the common-mode rejection due to differential detection, and the overall Q amplification of the sense signal by driving the device on resonance.

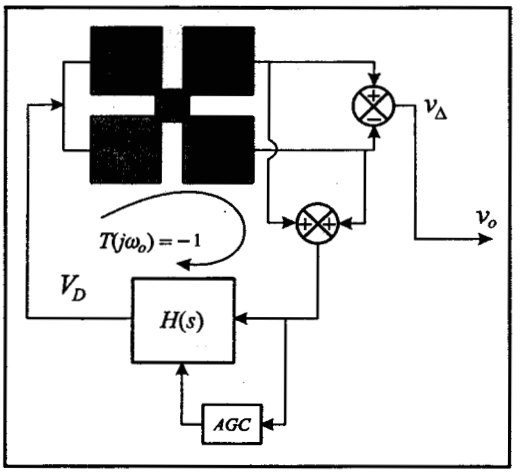

Figure 3. Block diagram of closed-loop electronics with JPL's MEMS-based microgyroscope.

Test results for current microgyroscope designs are shown in Figures 2 and 3. A Green chart is shown in Figure 3. The Green chart represents the standard deviation of a rotation rate measurement (square root of the Allan variance [ref] as a function of time. From this chart, a bias stability of 9 degrees/hr, a random angle walk of 1.5 deg/rt hr.

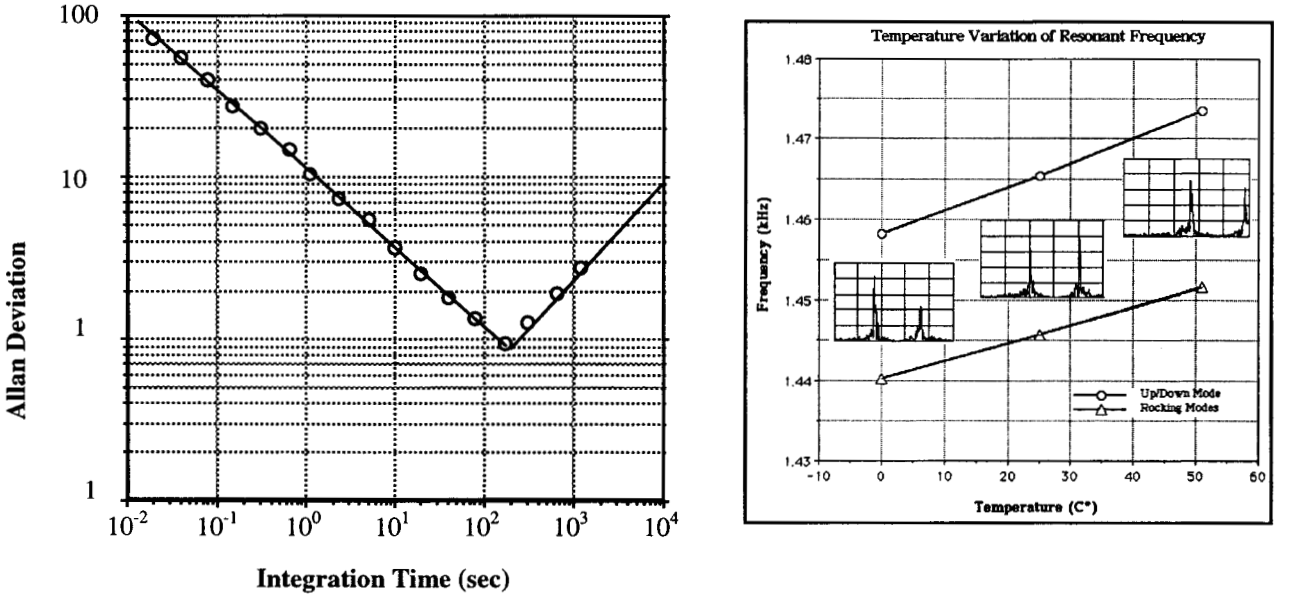

Figure 4. Rate Green Chart of JPL's microgyroscope is a plot of the standard deviation (square root of the Allan variance) as a function of integration time. The bias stability is 9 degrees/hr. The angle random walk (white noise) is 1.5 deg/rt hr.

5. THE FUTURE: "SYSTEM ON A CHIP"

1. Introduction

The future of micro- and nano-spacecraft may ultimately lie in what many are calling "System-On-A-Chip" (SOAC). At JPL, a SOAC program has been developed to produce an autonomous avionics system that integrates a central processing unit, memory storage, power management and distribution, telecommunications system, and sensors/actuators on a single silicon chip. Integration of these subsystems is scheduled to reach single-chip format in the 5-10 year time frame. A second generation SOAC is shown in Figure S1. This chip was fabricated on MIT's Lincoln Laboratory SOI CMOS line, and is 2.6 mm on a side. Applications such as microprobes, nanorovers, and aerobots will all benefit from the mass, volume, and power reductions associated with these developments. In addition, intellectual property (IP) and function-specific libraries will be available for use is subsequent missions; offering the system engineer access to capable MEMS-based micro analytical labs and/or control systems.

There are many challenges in SOAC development. For example, design techniques and tools need to be developed to accommodate digital, analog, mixed signal, RF communication, and MEMS on a single chip. Likewise system simulations need to model thermal, mechanical, and electrical characteristics of a system which includes not only those components listed above, but also an integrated package, telecommunications, power and power management, and potentially multiple material systems. Miniature power sources, and ultra low power devices and architectures likewise require revolutionary technology leaps. Testing, packaging and reliability are critical when the entire system resides on a single chip.

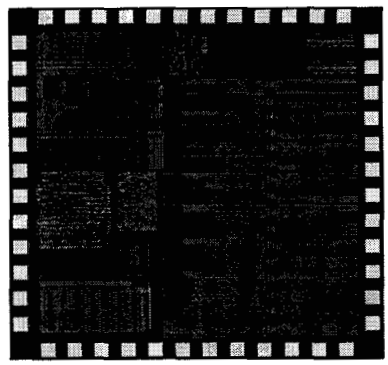

Figure S1. Design simulations of JPL's second generation System On A Chip.

2. MEMS-based RF Communications

One of the most challenging tasks in SOAC is the miniaturization and integration of an RF communications system. In conjunction with researchers at the University of Michigan, JPL has demonstrated several components of a planar, silicon micromachined, fully integrated, ultra low mass/volume RF front-end for X, K, and Ka-bands (10-40 GHz). The size reduction possible with a MEMS approach is shown in Figure S2. Note for example that the RF front-end of the Cassini spacecraft requires a footprint covering three bays. The future RF communications system on a chip requires 300g and 38 cm^3.

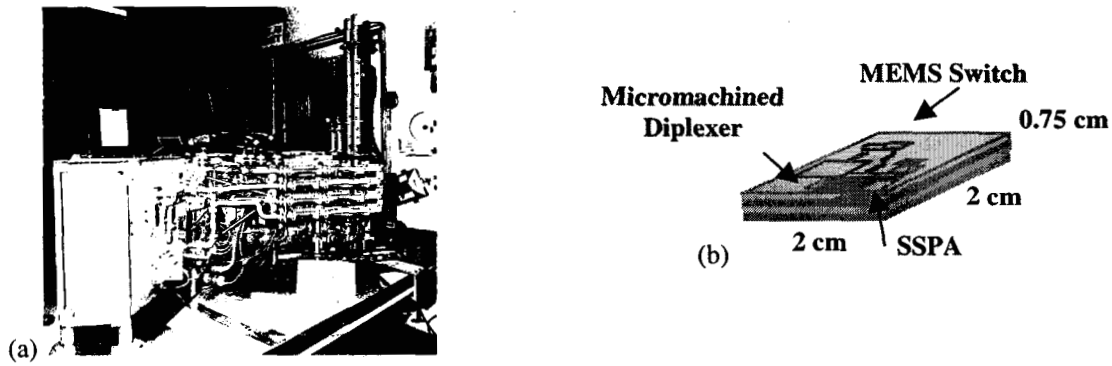

Figure S2 Present and future RF front-end technologies: (a) Cassini RF front-end takes up 3 bays while JPL's MEMS-based front-end is has a projected volume of 38 cm^3.

A closer look at current RF technology based on waveguides is shown in Figure S3 that includes a schematic of the RF front-end. The X-band front-end shown here has a mass of ~3.6 kg, and the total volume is ~2870 cm^3.

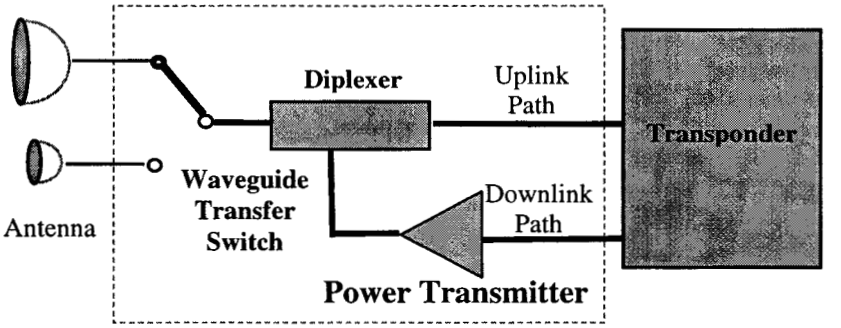

(a)

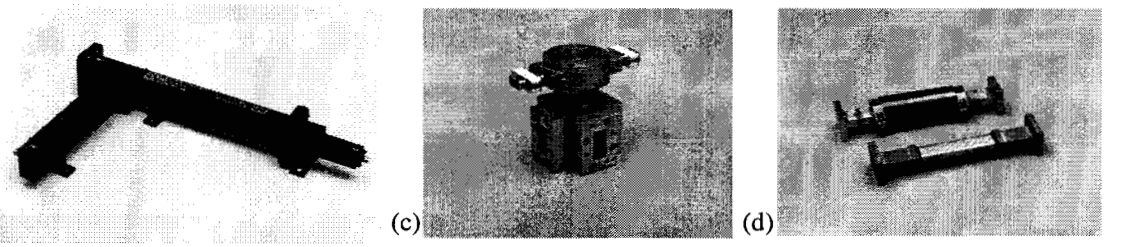

(b) (c) (d)

Figure S3 Examples of RF components in present-day spacecraft communications systems. (a) Schematic of X-Band front-end and (b) corresponding X-band Diplexer: long dimension = 40.6 cm; (c) X-Band Waveguide Transfer Switch (WTS), vertical dimension = 10.5 cm; and (d) Waveguide High- Frequency Transmission Line Technology: Shorter dimension is 10.5 cm

A fully integrated, ultra low mass/volume front-end fabricated using silicon micromachining technology can be built with a chip size of 38 cm^3, and a mass of <300g. In this design, circuit components are integrated in a silicon multi-layered structure with micromachined, self-packaged interconnections. MEMS developments which allow this drastic miniaturization includes a MEMS transfer switch, and micromachined resonator cavities for IF downconversion filters and diplexers. (Si/Ge power transmitters complete the miniaturized design, but will not be addressed here. However, integration of several material systems and vertical MEMS building blocks re-emphasizes the needs for parallel efforts in reliability, packaging and flight qualification.)

A schematic and corresponding SEM of the University of Michigan's K-band switch are shown in Figure S4.[S1, S2] The device is fabricated above a finite-ground coplanar waveguide (FGCPW) line [S3] and is designed in a single-pole, double-throw configuration to minimize vibration and shock effects. Insertion losses of <0.2 dB at 20 GHz have been demonstrated with a serpentine spring configuration. Likewise, this with this technology, isolation values of 30 dB up to 40 GHz are possible. Pull-in voltages, on the order of 14 V, are being reduced with improved spring designs.

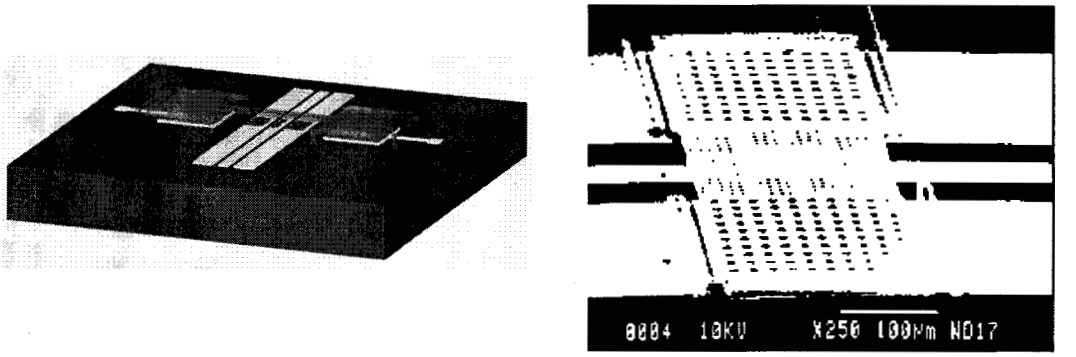

Figure S4 Schematic and SEM of University of Michigan's MEMS K-band switch, operating

In addition to RF switching technology, micromachined High-Q resonators have been developed. An example of this technology is shown schematically in Figure S5 in #-D and cross-sectional views. These resonators have been demonstrated with Q's over 80,000 [S4} and a center frequency temperature coefficient of -10 ppm/°C. Two-resonator bandpass filters have also been demonstrated [S2] up to 14.5 MHz insertion losses <1 dB, and % bandwidths of ~0.2%. This approach is very promising in replacing conventional filters and diplexers in RF front-ends.

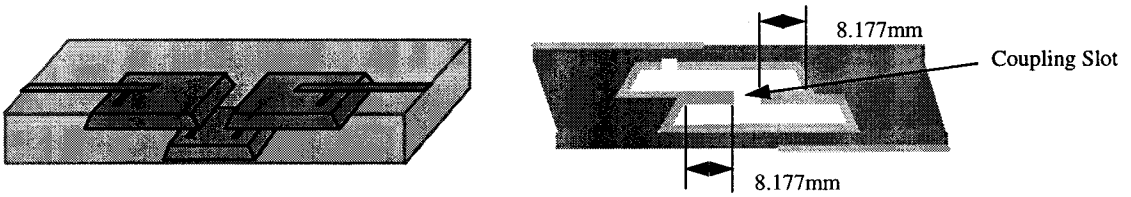

Figure S5. 3-D and cross-sectional schematics of University of Michigan's micromachined resonator cavities.

The MEMS-based RF front-end will reduce current technology by a factor of 12X in mass, and a factor of 70X in volume over conventional waveguide technologies. This enables lower cost missions, and ultimately produces an entire system on a chip (SOAC).

6. CONCLUSIONS

The reduction of mission costs requires substantial reductions in mass, volume, and power consumption. At the same time, ever-more ambitious science objectives require miniaturization without loss of performance. MEMS enable this exploration of space by producing miniature science and engineering devices that are potentially integrable with radiation-hardened electronics. Reliability, packaging and flight qualification of MEMS and their related systems are critical in fast insertion of these breakthrough EMS technologies into space applications. The international space and MEMS communities recognize this, and large efforts are being created to produce an exciting new era in space exploration.

7. ACKNOWLEDGEMENTS

The author thanks the following people for their support in this endeavor: Steve Manion of Mars Microprobe, Perry Danish of JPL's mission assurance group, Tim Krabach, Tony Tang, Elizabeth Kolawa, Rita Wilcoxin, Sam Kayali, Richard Kemske, Randy Blue, and William Tang. The JPL work presented in this paper was performed by the Jet Propulsion Laboratory, California Institute of Technology, ~~and was sponsored by~~ under a contract the National Aeronautics and Space Administration, Office of Space Access and Technology.

8. REFERENCES

16460

R1. B. Stark, "MEMS Reliability Assurance Guidelines for Space Applications," JPL D-~~xxxx~~, Jet propulsion Laboratory, October 30, 1998.

R2. M. Tabib-Azar, K. Wong, and W. Ko, "Aging Phenomenon in heavily doped (p+) micromachined silicon cantilever beams," *Sensors and Actuators A.*, Vol. 33, pp. 199-206, 1992.

R3. R. Maboudian, and R. T. Howe, "Critical Review: Adhesion in Surface Micromechanical Structures," *J. Vac. Sci. and Technol. B*, Vol. 15, Jan. 1997.

R4. L. D. Edmonds, C. I. Lee, G. M. Swift, "Radiation Response of MEMS Accelerometer: An Electrostatic Force," 1998 National Space and Radiation Effects conference, July 20-24, 1998.

R5. A. R. Knudson, S. Buchner, P. McDonald, W. J. Stapor, A. B. Campbell, K. S. Grabowski, D. L. Knies, S. Lewis, and Y. Zhao, "The Effects of Radiation on MEMS Accelerometers," IEEE *Trans. on Nuclear Sci.*, Vol. 43, pp. 3122-3125, December, 1996.

R6. C. Marxer, M.-A. Gretillat, N. F. de Rooij, R. Battig, O. Anthamatten, B. Valk, P. Vogel, "Reliability considerations for electrostatic polysilicon actuators using as and example the REMO components," *Sensors and Actuators A.*, Vol. 61, pp. 449-454, 1997.

R7. J. Kloeser, E. Zake, F. Bechtold, and H. Reichl, "Reliability Investigations of Fluxless Flip-Chip Interconnections on Green Tape Ceramic Substrates," IEEE Trans. Components, packaging, and Manufacturing Technology, Part A, Vol. 19, No. 1, pp. 24-33, March 1996.

R8. W. Daum, W. Burdick Jr., and R. Filtion, "Overlay high-density interconnect: A chips-first multichip model technology," IEEE Computer, Vol. 26, No. 4, pp. 23-29, April 1993.
R9. J. Butler, V. Bright, and J. Comtois, "Advanced multichip module packaging of mciroelectromechanical systems, "Tech. Digest of the 9th Internat. Conf. On Solid-State Sensors and Actuators (Transducers '97), Vol. 1, pp. 261-264, June 1997.
R10. R. Filtion, R. Wojnarowski, R. Saia, and D. Kuk, "Demonstration of a chip scale chip-on-flex technology," Proc. Of the 1996 Internat. Conf on Multichip Modules, SPIE Vol. 2794, pp. 351-356, 1996.
R11. MUMPS

[G1] T.K.Tang, R.C.Gutierrez, J. Wilcox, C. Stell, V. Vorperian, R. Calvet, W. Li, I. Charkaborty, R. Bartman, W. Kaiser, " Silicon Bulk Micromachined Vibratory Gyroscope", Tech Digest, Solid-State Sensor and Actuator Workshop, Hilton Head, S.C. pp.288-293, June 1996.
[G2] M. Weinberg, J. Bernstein, J. Borenstein, J. Campbell, J. Cousens, B. Cunningham, R. Fields, P. Greiff, B. Hugh, L. Niles, J. Sohn, "Micromachining inertial instruments", SPIE Vol. 2879, pp.26-36, September 1996.
[G3] P. B. Ljung, T. N. Juneau, and A. P. Pisano, "Micromachined Two Input Axis Angular Rate Sensor", *Proceedings of the ASME Dynamic Systems and Control Division,* DSC-Vol. 57-2, IMECE/ASME, pp.957-962, 1995.
[G4] M.Putty, K. Najafi, "A Micromachined Vibratory Ring Gyroscope", Tech Digest, Solid-State Sensor and Actuator Workshop, Hilton Head, S.C., pp.213-220, June 1994.
[G5] " Micro-IMU for space applications," 1998 GOMAC and HEART Conference, Arlington, Virginia, March 17-20, 1998.
[G6] " Micro Inertial Reference System on-a-Chip," 1998 WestCon, Anaheim, CA, September 15-17, 1998.

[S1] S. Pacheco, C. T.-C. Nuygen, and L. P. B. Katehi, "Micromechanical Electrostatic K-Band Switches," *IEEE MTT-S Digest*, pp. 1569-1572, 1998.
[S2] L. P. B. Katehi, G. M. Rebeiz, and C. T.-C. Nuygen, "MEMS and Si-micromachined Components for Low-Power, high Frequency Communications Systems," *IEEE MTT-S Digest*, pp. 331-333, 1998.
[S3] F. Brauchler, S. Robertson, J. East, and L. P. B. Katehi, "W-Band, Finite Ground Coplanar (FGC) Line Circuit Elements," *IEEE MTT-S Digest*, pp. 1141-1144, 1996.
[S4] C. T.-C. Nuygen, "High-Q micromechanical oscillators and filters for communications (invited)," 1997 IEEE Internat. Symp. on Circuits and Systems, Hong Kong, June 9-12, 1997, pp. 2825-2828.

Figure 9. 3-D and cross-sectional schematics of University of Michigan's micromachined resonator cavities.

The MEMS-based RF front-end system can potentially reduce current systems by a factor of 12 in mass, and a factor of 70 in volume over conventional waveguide technologies. By producing a MEMS-based communications system, an entire autonomous avionics system can be integrated on a monolithic cube structure. Future advances in submicron design rules, mixed signal electronics, robust MEMS devices, MEMS interconnection technology, ultra-low power electronics, micro-power sources, revolutionary system packaging, system designs for harsh environments, reliability and flight testing of a fully integrated system architecture will enable SOAC technology in space applications. Each component is a research project. However, SOAC development ultimately enables new classes of network science and nano-missions.

6. CONCLUSIONS

The reduction of mission costs requires substantial reductions in mass, volume, and power consumption. At the same time, increasingly ambitious science objectives require miniaturization without loss of performance. MEMS enable this exploration of space by producing miniature science and engineering devices that are potentially integrable with radiation-hardened electronics. Reliability, packaging and flight qualification of MEMS and their related systems are critical in fast insertion of breakthrough MEMS technologies into space applications. The international space and MEMS communities recognize this, and great efforts are being directed towards producing an exciting new era in space exploration.

ACKNOWLEDGEMENTS

The author wishes to thank the following JPL personnel for their contribution in this endeavor: Steve Manion, Randy Blue, Steve Vargo, Tony Tang, William Tang, Elizabeth Kolawa, Martin Herman, Brent Blaes, Leon Alkalai, Perry Danish, Tim Krabach, Rita Wilcoxin, Sam Kayali, and Richard Kemske. The JPL work presented in this paper was performed by the Center for Integrated Space Microsystems, and the Center for Space Microelectronics Technology, Jet Propulsion Laboratory, California Institute of Technology, and under a contract with the National Aeronautics and Space Administration.

REFERENCES

1. W. C. Tang, "Micromechanical Devices at JPL for Space Exploration," Proc. Of the 1998 IEEE Aerospace Conf., Mar 21-28, 1998, Snowmass, Colorado.
2. De Aragon, A. M., "Space applications of micro/nano-technologies," J. Micromechanics and Microengineering, Vol. 8, No. 2, pp. 54-56, 1998.
3. J. Benoit , "Micro and Nanotechnologies - A Challenge on the Way Forward to New Markets," Mat. Sci. and Engineering B Solid State Mater. For Adv. Technol., Vol. 51, No. 1-3, pp. 254-257, 1998.
4. L. Muller, M. Hecht, L. M. Miller, and H. K. Rockstad, "Packaging and Qualification of MEMS-Based Space Systems," *Tech. Dig. IEEE Int. Workshop on Micro Electro Mechanical Systems*, pp. 503-508, San Diego, CA (1996).
5. T.K.Tang, R.C.Gutierrez, C. Stell, V. Vorperian, K. Shcheglov, L. M. Miller, J. A. Podosek, W. J. Kaiser, " Micro-IMU for space applications," 1998 GOMAC and HEART Conference, Arlington, Virginia, March 17-20, 1998.
6. A. Partridge, J. K. Reynolds, B. W. Chui, E. M. Chow, A. M. Fitzgerald, L. Zhang, S. R. Cooper, T. W. Kenny, and N. I. Maluf, "A High Performance Piezoresistive Accelerometer," Proc. Of Solid-State Sensor and Actuator, Hilton Head, SC, pp. 59-64, June 1998.
7. L. M. Miller, J. A. Podosek, E. Kruglick, T. W. Kenny, J. A. Kovacich, and W. J. Kaiser, "A μ-Magnetometer Based on Electron Tunneling," *Proc. Micro Electro Mechanical Systems*, pp. 467-471, San Diego, CA (1996).

8. W. T. Pike, R. D. Martin, W. J. Kaiser, and W. B. Banerdt, "Development of microseismometers for space applications," Ann. Geophys., Vol. 14, pp. C828, 1996.
9. D. Crisp, W. J. Kaiser, T. R. VanZandt, M. E. Hoenk, J. E. Tillman, "Micro Weather Stations for Mars," Acta Astronautica, Vol. 35, pp. 407-415, 1995.
10. S. E. Vargo, E. P. Muntz, G. R. Shilett, W. C. Tang, "The Knudsen Compressor as a Micro and Macroscale Vacuum Pump Without Moving Parts or Fluids," 45th American Vacuum Soc. International Symp., Baltimore, MD Nov 2-6, 1998
11. F. V. Steenkiste, K. Baert, D. Debruyker, V. Spiering, B. van der Schoot, P. Arquint, R. Born, and K. Schumann, "A microsensor array for biochemical sensing," Sensors and Actuators B, Vol. 44, pp. 409-412, 1997.
12. D. V. Wiberg, M. H. Hecht, O. J. Oreient, A. Chutjian, K. Yee, and S. Fuerstenau, "A LIGA fabricated quadrupole array for mass spectroscopy," Ext. Abs., High Aspect Ration Micro Structure Tech Forum, Madison, WI, 1997.
13. J. Mueller, W. C. Tang, A. P. Wallace, W. J. Li, D. P. Bame, I. Chakraborty, and R. A. Lawton, "Design, analysis, and fabrication of a vaporizing liquid micro-thruster," Proc. AIAA/ASME/SAE/ASEE Joint Prop. Conf., Seattle, WA, 1997, AIAA 97-3054.
14. L. P. B. Katehi, G. M. Rebeiz, and C. T.-C. Nuygen, "MEMS and Si-micromachined Components for Low-Power, high Frequency Communications Systems," *IEEE MTT-S Digest*, pp. 331-333, 1998.
15. B. Stark, "MEMS Reliability Assurance Guidelines for Space Applications," JPL internal document, JPL D-16460, October 30, 1998. For further information, contact Sam Kayali at skayali@pop.jpl.nasa.gov.
16. M. Tabib-Azar, K. Wong, and W. Ko, "Aging Phenomenon in heavily doped (p+) micromachined silicon cantilever beams," *Sensors and Actuators A.*, Vol. 33, pp. 199-206, 1992.
17. R. Maboudian, and R. T. Howe, "Critical Review: Adhesion in Surface Micromechanical Structures," *J. Vac. Sci. and Technol. B*, Vol. 15, Jan. 1997.
18. L. D. Edmonds, C. I. Lee, G. M. Swift, "Radiation Response of MEMS Accelerometer: An Electrostatic Force," 1998 National Space and Radiation Effects conference, July 20-24, 1998.
19. J. Kloeser, E. Zake, F. Bechtold, and H. Reichl, "Reliability Investigations of Fluxless Flip-Chip Interconnections on Green Tape Ceramic Substrates," IEEE Trans. Components, packaging, and Manufacturing Technology, Part A, Vol. 19, No. 1, pp. 24-33, March 1996.
20. T. K. Tang, R.C.Gutierrez, C. B. Stell, V. Vorperian, G. A. Arakaki, J. T. Rice, W. J. Li, I. Chakraborty, K. Shcheglov, and J. Wilcox, "A packaged silicon MEMS vibratory gyroscope for microspacecraft," Proc. IEEE Micro Electro Mech. Sys. Workshop, Nagoya, Japan, pp. 26-30, 1997.
21. L. Alkalai and E. Kolawa, "Systems-On-A-Chp for Space Applications," to be presented at STAIF-99, FL, Feb, 1999.
22. S. Pacheco, C. T.-C. Nuygen, and L. P. B. Katehi, "Micromechanical Electrostatic K-Band Switches," *IEEE MTT-S Digest*, pp. 1569-1572, 1998.
23. F. Brauchler, S. Robertson, J. East, and L. P. B. Katehi, "W-Band, Finite Ground Coplanar (FGC) Line Circuit Elements," *IEEE MTT-S Digest*, pp. 1141-1144, 1996.